

1 **Coral epigenetic responses to nutrient stress: histone H2A.X phosphorylation dynamics and DNA**
2 **methylation in the staghorn coral *Acropora cervicornis***

3

4 Javier Rodriguez-Casariago ¹, Mark Ladd ², Andrew Shantz ², Christian Lopes ³, Manjinder S. Cheema ⁴,
5 Bohyun Kim ⁴, Steven Roberts ⁵, James W. Fourqurean ³, Juan Ausio ⁴, Deron E. Burkepile ², Jose Eirin-
6 Lopez ^{1,*}

7

8 ¹Environmental Epigenetics Laboratory, Institute of Water and Environment, Department of Biological
9 Sciences, Florida International University, Miami FL, USA.

10 ²Department of Ecology, Evolution and Marine Biology, University of California, Santa Barbara CA, USA.

11 ³Seagrass Laboratory, Institute of Water and Environment, Department of Biological Sciences, Florida
12 International University, Miami FL, USA.

13 ⁴Department of Biochemistry and Microbiology, University of Victoria, Victoria BC, Canada.

14 ⁵School of Aquatic and Fishery Science, University of Washington, Seattle WA, USA.

15

16 * Corresponding author: Marine Sciences Program, Florida International University, Biscayne Bay

17 Campus, 3000 NE 151 Street, office MSB-360, North Miami, FL 33181, USA. Email: jeirinlo@fiu.edu,

18 Phone: 305-919-4000

19

20

21 **Running Title:** Coral epigenetic responses to nutrient stress

22

23 **Abstract**

24 Nutrient pollution and thermal stress constitute two of the main drivers of global change in the coastal
25 oceans. While different studies have addressed the physiological effects and ecological consequences of
26 these stressors in corals, the role of acquired modifications in the coral epigenome during acclimatory and
27 adaptive responses remains unknown. The present work aims to address that gap by monitoring two
28 types of epigenetic mechanisms, namely histone modifications and DNA methylation, during a seven
29 week-long experiment in which staghorn coral fragments (*Acropora cervicornis*) were exposed to nutrient
30 stress (nitrogen, nitrogen + phosphorus) in the presence of thermal stress. The major conclusion of this
31 experiment can be summarized by two main results: First, coral holobiont responses to the combined
32 effects of nutrient enrichment and thermal stress involve the post-translational phosphorylation of the
33 histone variant H2A.X (involved in responses to DNA damage), as well as non-significant modifications in
34 DNA methylation trends. Second, the reduction in H2A.X phosphorylation (and the subsequent potential
35 impairment of DNA repair mechanisms) observed after prolonged coral exposure to nitrogen enrichment
36 and thermal stress is consistent with the symbiont-driven phosphorus limitation previously observed in
37 corals subject to nitrogen enrichment. The alteration of this epigenetic mechanism could help to explain
38 the synergistic effects of nutrient imbalance and thermal stress on coral fitness (i.e., increased bleaching
39 and mortality) while supporting the positive effect of phosphorus addition to improving coral resilience to
40 thermal stress. Overall, this work provides new insights into the role of epigenetic mechanisms during
41 coral responses to global change, discussing future research directions and the potential benefits for
42 improving restoration, management and conservation of coral reef ecosystems worldwide.

43

44

45

46 **Key Words:** Global change, pollution, cnidarians, acclimatization, histones, DNA methylation.

47 **INTRODUCTION**

48 Hermatypic (i.e., reef-building, stony) corals constitute the structural basis of reef ecosystems, providing
49 the foundation for over 25% of marine and coastal biodiversity. Unfortunately, during the last decades,
50 coral reefs have experienced dramatic declines worldwide, caused by local and global anthropogenic
51 stressors (Pandolfi et al., 2003). The sessile lifestyle and long lifespan of corals increase their vulnerability
52 to a rapidly changing environment (Cunning & Baker, 2012; Nesa & Hidaka, 2009), but also support the
53 idea that their evolutionary success relies on a remarkable level of phenotypic plasticity (Barshis et al.,
54 2013; Bruno & Edmunds, 1997; Dimond & Roberts, 2016; Dixon, Bay, & Matz, 2014). Although a high
55 degree of genotypic diversity can be found in some coral species (Ayre & Hughes, 2000, 2004; Souter,
56 2010), it is becoming increasingly clear that the plasticity provided by this mechanism will not be enough
57 to keep up with the rapid progression to a warmer, more polluted, more acidic and carbonate-limited
58 ocean (Hoegh-Guldberg et al., 2007; Hughes et al., 2017). Such a dark perspective has sparked the
59 interest for the study of environmentally acquired nongenetic modifications (i.e., microbiome and
60 epigenome dynamics) in these organisms, given their intrinsic potential to increase coral acclimatization
61 and adaptation rates under rapidly changing environments (Palumbi, Barshis, Taylor-Knowles Nikki, &
62 Bay, 2014; van Oppen, Oliver, Putnam, & Gates, 2015). For instance, recent reports have revealed that
63 specific symbiont strains can provide corals with higher tolerances to thermal stress (Leal et al., 2015;
64 Silverstein, Cunning, & Baker, 2015, 2017), and that coral responses to different drivers of global climate
65 change do in fact involve changes in the epigenome (i.e., DNA methylation) (Beal, Rodriguez-Casariago,
66 Rivera-Casas, Suarez-Ulloa, & Eirín-López, 2018; Eirin-Lopez & Putnam, 2019; Liew et al., 2018; Putnam,
67 Davidson, & Gates, 2016)

68
69 Organismal responses to environmental changes involve the activation of different mechanisms operating
70 at diverse levels, from early genetic responses (Hoffmann & Willi, 2008) to whole-individual physiological
71 responses (Boyd et al., 2015; Shultz et al., 2014). While different, all these mechanisms invariably require
72 the modulation of the expression of specific sets of genes, promoting dynamic and sometimes reversible
73 responses facilitating the onset of acclimatized phenotypes (Stillman & Armstrong, 2015). Epigenetic

74 modifications, defined as phenomena and mechanisms that cause heritable (both mitotically and/or
75 meiotically) chromosome-bound changes to gene expression, not involving changes to DNA sequence
76 (*sensu* Deans & Maggert, 2015), are at the center of this regulatory process (Eirin-Lopez & Putnam,
77 2019). Among the different epigenetic mechanisms known so far, DNA methylation is the most studied in
78 all types of organisms (Schübeler, 2015), including corals where recent studies have characterized DNA
79 methylation levels in the germline and evidenced the involvement of this mechanism in responses to
80 ocean acidification (Dimond & Roberts, 2016; Dixon et al., 2014; Liew et al., 2018; Marsh, Hoadley, &
81 Warner, 2016; Putnam et al., 2016). Yet, studies elucidating the links between DNA methylation and gene
82 expression, the interaction among different types of epigenetic mechanisms, as well as their precise
83 involvement in responses to different drivers of global climate change in ecologically and environmentally
84 relevant organisms, are still lacking (Beal et al., 2018).

85
86 Among the multiple threats posed by global change, anthropogenic nutrient pollution constitutes one the
87 major drivers of coral decline (Fabricius, 2005; Wagner, Kramer, & van Woesik, 2010; Wooldridge, 2009).
88 Their potential effects include increased coral bleaching (Cunning & Baker, 2012; Vega Thurber et al.,
89 2014; Wooldridge, 2009), disease (Zaneveld, McMinds, & Thurber, 2017), reduced growth rates (Dunn,
90 Sammarco, & LaFleur, 2012; Shantz & Burkepile, 2014) and impaired reproduction (Loya, Lubinevsky,
91 Rosenfeld, & Kramarsky-Winter, 2004). A possible mechanism underlying these deleterious effects is the
92 rapid proliferation of symbiont populations triggered by the disruption of the nitrogen (N)-limited
93 environment maintained by the coral host inside the symbiosome (Downs et al., 2002; Nesa, Baird, Harii,
94 Yakovleva, & Hidaka, 2012). The resulting phosphorus (P) starvation damages the photosynthetic
95 machinery and alters the ionic balance in the symbiont thylakoid membranes (Pogoreutz et al., 2017;
96 Wiedenmann et al., 2012), subsequently increasing the export of reactive oxygen species (ROS) to the
97 intracellular space while intensifying oxidative and DNA damage in both the host and the symbiont
98 (Baruch, Avishai, & Rabinowitz, 2005; Ezzat, Maguer, Grover, & Ferrier-Pagès, 2016; McGinty,
99 Pieczonka, & Mydlarz, 2012; Nesa et al., 2012; Saragosti, Tchernov, Katsir, & Shaked, 2010;
100 Wiedenmann et al., 2012). Overall, the effects of nutrient pollution will work synergistically with other

101 stressors (particularly thermal stress) increasing bleaching at a mechanistic level (Pogoreutz et al., 2017)
102 and coral mortality (Nesa & Hidaka, 2009; Yakovleva et al., 2009).

103
104 Although the potential ways in which nutrient and thermal stress can affect corals are well studied (Brown,
105 1997; D'Angelo & Wiedenmann, 2014; Nielsen, Petrou, & Gates, 2018), the identity and the precise role of
106 the epigenetic mechanisms linked to acclimatory and adaptive responses to these stressors remains
107 unknown. In order to fill that gap, the present work conducted a field experiment consisting of two different
108 types of coral nutrient enrichments (treatment 1, nitrogen only; treatment 2, nitrogen + phosphorus) using
109 the staghorn coral *Acropora cervicornis* as model organism. Given that a thermal stress event was
110 observed in the study are at the same time that this experiment was taking place, the obtained results
111 provide a unique opportunity to analyze the synergies between both types of stress mediating epigenetic
112 responses in field conditions. Two types of epigenetic mechanisms were studied for that purpose,
113 including histone modifications [histone H2A.X phosphorylation also known as gamma-H2A.X, a histone
114 modification involved in DNA repair and a universal marker of DNA damage (González-Romero et al.,
115 2012; Maré Chal & Zou, 2013)] and DNA methylation. It is hypothesized that nutrient enrichment will
116 accelerate the growth of the symbiont population within the holobiont, resulting in a higher production of
117 ROS which will in turn cause DNA damage, triggering an increase in gamma-H2A.X (associated to DNA
118 repair activation) and changes in DNA methylation. It is also hypothesized that gamma-H2A.X formation
119 will be impaired in corals exposed only to N enrichment (treatment 1), due to the P limitation caused by
120 proliferation of symbionts in the absence of a P supply. Consequently, corals subject to N enrichment
121 (treatment 1) would be expected to experience lower levels of DNA repair, encompassing deleterious
122 phenotypic effects.

123

124 **METHODS**

125

126 *Study Site, Experimental and Sampling Design*

127 Nutrient exposures were conducted using a common garden experiment in a large sand flat located near
128 Pickles Reef in the Upper Florida Keys, Key Largo, FL (Fig. 1A) (25° 00' 05" N, 80° 24' 55" W) in
129 approximately 5 - 7 m depth of water. Ambient nutrient conditions are relatively oligotrophic at this site
130 (dissolved inorganic nitrogen (DIN) < 1.2 µM, soluble reactive phosphorus (SRP) < 0.04 µM; Zaneveld et
131 al., 2016), making it a suitable location to test the effects of nutrient enrichment on corals. A total of 144
132 fragments of the staghorn coral *Acropora cervicornis* (three parental colonies, 7 to 13 cm in length) were
133 obtained from a nearby offshore coral nursery operated by the Coral Restoration Foundation (permit no:
134 FKNMS 2014-071). Each coral fragment was secured to a 50 cm tall section of PVC tubing (4 cm
135 diameter) set in a base of concrete using nylon cable ties, for a total of 12 fragments per stand (Fig. 1B,
136 C). Twelve experimental stands were distributed in a randomized block design across the study area with
137 ≥ 2 m separation between them. Each stand (n = 4 per treatment) was randomly assigned to one of three
138 treatment conditions as follows: Control (Ctrl), nitrogen enrichment (N), and nitrogen + phosphorous
139 enrichment (N+P). Controls were replicated in the same way treatments were, to account for the potential
140 environmental variability typical of field experiments. Coral fragments attached to stands were allowed to
141 acclimate for more than 10 days without treatment until any visible wounds resulting from the
142 fragmentation process healed. N enrichment was achieved using Florikan 0-19-0 slow release ammonium
143 nitrate fertilizer (300 g) as detailed by (Vega Thurber et al., 2014); N+P enrichment was obtained by
144 combining 0-19-0 slow release ammonium nitrate fertilizer (300 g) with 80 g of 40-0-0 slow release Super
145 phosphate fertilizer. Ctrl stands were not exposed to any nutrient source. In both N and N+P treatments,
146 nutrient exposure was achieved through the diffusion of nutrients in water by evenly dividing the fertilizer
147 into two perforated PVC tubes, wrapped in mesh and secured at opposing sides of each block via cable
148 ties. This method was previously validated to triplicate the ambient levels of DIN and SRP for a period of
149 30 - 45 days in similar conditions (Heck, Pennock, Valentine, Coen, & Sklenar, 2000; Sotka & Hay, 2009;
150 Vega Thurber et al., 2014).

151
152 Epigenetic modifications in invertebrates can occur rapidly after exposure to environmental stress
153 (Gonzalez-Romero et al., 2017; Rivera-Casas et al., 2017; Suarez-Ulloa, Gonzalez-Romero, & Eirin-
154 Lopez, 2015). Therefore, coral fragments were sampled at three different times during day 1 of exposure
155 (1 h, 2 h, 5 h), day 2, day 7, and weekly thereafter for the next 4 weeks. For each sample, one coral
156 fragment was randomly collected from each stand (n = 4 coral fragments per treatment, n = 12 fragments
157 per sampling). Fragments were collected by cutting the cable ties securing them to the stands and were
158 subsequently stored in individual sealed sterile plastic bags. Once all samples were collected, bags were
159 transported to the surface and immediately flash-frozen in liquid nitrogen. Fragments were divided into
160 sub-samples for nutrient analyses and for molecular analyses, finally stored at -80 °C.

161

162 *Nutrient Quantification*

163 N and P content were quantified in tissue from coral fragments collected during the experiment, including
164 increased sampling frequency during week 1. This sampling design is consistent with the findings of
165 Achituv, Ben-Zion, & Mizrahi (1994) and Muller-parker, Cook, & D'Elia, (1994), suggesting that the most
166 significant nutrient changes in coral tissue occur within that period. Coral holobiont (the unit formed by the
167 coral animal and its associated microorganisms consisting of bacteria, archaea, fungi, viruses, and protists
168 including Symbiodiniaceae dinoflagellate algae) tissue was removed from a portion of each of the
169 fragments sampled using an airbrush loaded with ultrapure water, and was dried to a constant weight at
170 60 °C and homogenized to powder. Samples were subsequently fumed with HCl for 14 days to completely
171 remove the skeletal inorganic carbon fraction (Szmant et al. 1990) and dried at 70 °C until no further
172 weight change was observed. Carbon (C) and N content were measured in aliquots (10 mg) of dried and
173 decalcified tissues using a FISONs elemental analyzer (NA1500, Loughborough, UK). P content was
174 analyzed *sensu* Solórzano & Sharp, (1980) using a modification adapted for tissue (Fourqurean, Zieman,
175 & Powell, 1992). Briefly, 5 to 10 mg of dried tissue were placed into glass scintillation vials, diluted with 0.5
176 mL of 0.17 M Na₂SO₄ and 2 mL of 0.017 M MgSO₄, and dried again at 90 °C. The resulting powder was
177 incubated at 500 °C for 3 h and cooled down to room temperature. A total of 5 mL of 0.2 N HCl was added

178 to these oxidized and dried samples and incubated at 80 °C for 30 min, after which they were diluted with
179 10 mL of deionized water and allowed to stand overnight for the insoluble ash to settle. The phosphate
180 concentration in the solution was determined as SRP using a colorimetric assay. The elemental content
181 was calculated on a percentage of dry weight basis, and elemental ratios were calculated on a mole:mole
182 basis. Data was collected following time frames reported in the literature, greater than or equal to 10 days
183 (Godinot, Houlbrèque, Grover, & Ferrier-Pagès, 2011) but less than 8 weeks (Godinot, Ferrier-Pagès, &
184 Grover, 2009), while considering the rapid initial changes accounted in the sampling design (Achituv et al.,
185 1994; Gisèle Muller-Parker et al., 1994). Accordingly, samples for the first three days were used as initial
186 time (T1) and then organized into samples greater than 10 days but less than 8 weeks (T2 and T3) to
187 ensure nutrient uptake representation.

188

189 *Symbiont Density Analysis*

190 The density of coral symbiont (Symbiodiniaceae) algae was quantified across treatments and exposure
191 times by removing all tissue from the coral skeleton using the procedure detailed above. Upon extraction,
192 tissue samples were homogenized using a tissue grinder and centrifuged for 5 minutes using a hand
193 centrifuge to isolate symbiont cells. Each sample was subsequently divided into five technical replicates
194 (100-300 µL each) and symbiont cells were quantified using a hemocytometer (Weber Scientific,
195 Hamilton, NJ) in an inverted microscope (Leica, Buffalo Grove, IL). The extracted fragment's surface area
196 (cm²) was estimated using the aluminum foil method (J. Marsh, 1970). Quantifications were averaged
197 across technical replicates to produce mean symbiont density (cells x cm⁻²) for each fragment. To
198 determine whether enrichments impacted *Symbiodinium* growth rates, we tested for differences in
199 the *Symbiodinium* density through time within each of the three treatments. To do so, we used linear
200 mixed effects models with hours since enrichment began as a continuous predictor and included growth
201 platform as a random factor to account for non-independence within the platforms (using χ^2 with 1 d.f. to
202 test whether symbiodinium growth rate significantly differs from zero through time). Tests were conducted
203 using the nlme package in R (Pinheiro et al. 2018). Normality and homogeneity of variance were
204 confirmed via quantile-quantile plots and plots of fitted versus residual values.

205

206 *Histone Isolation, Separation and Detection*

207 Histone proteins re isolated as described elsewhere and adapted to coral tissue in the present work
208 (Rivera-Casas et al., 2017). Accordingly, 5 mg of holobiont tissue were homogenized in a buffer consisting
209 of 100 mM KCl, 50 mM Tris-HCl, 1 Mm MgCl₂ and 0.5% Triton X-100 (pH 7.5) and containing a protease
210 inhibitor mixture. After homogenization and incubation on ice for 5 min, samples were centrifuged at
211 12,000 g for 10 min at 4 °C. The resulting pellets were re-suspended in 0.6 N HCl, homogenized, and
212 centrifuged again. The supernatant extracts were precipitated with six volumes of acetone at -20 °C
213 overnight and centrifuged at 12,000 g for 10 min at 4 °C. The acetone pellets were dried using a Vacufuge
214 concentrator (Eppendorf, Hamburg, Germany), and stored at -80 °C. Histone protein separation was
215 carried out in SDS-PAGE gels using ClearPAGE SDS gels 4-20% (C.B.S. Scientific, Del Mar, CA). Gels
216 were stained with 0.2% (w/v) Coomassie blue in 25% (v/v) 2-propanol, 10% (v/v) acetic acid, and de-
217 stained in 10% (v/v) 2-propanol, 10% (v/v) acetic acid. Additional histone separation was carried out using
218 High Performance Liquid Chromatography (HPLC) as described in Rivera-Casas et al. (2017). Histone
219 proteins were detected using commercial antibodies in western-blot analyses, including anti-H2A.X
220 (H2A.X.ab, Abcam Cambridge, MA; H2A.Xry, Raybiotech, Norcross, GA) and anti-γH2A.X (γ-H2A.X ab,
221 Rockland, Pottstown, PA; γ-H2A.Xry, Raybiotech, Norcross, GA). SDS-PAGE gels were electro-
222 transferred to a nitrocellulose membrane (C.B.S. Scientific , Del Mar, CA) and processed as described
223 elsewhere (Rivera-Casas et al., 2017). Membranes were incubated with a secondary goat anti-rabbit
224 antibody (Rockland, Pottstown, PA) that was subsequently detected using enhanced chemiluminescence
225 (Amershan ECL Prime Western Blotting Detection Reagent, GE Healthcare Life Sciences, Piscataway,
226 NJ). Results were analyzed using the ChemiDoc-It TS2 Imager image analysis system (UVP Inc., San
227 Gabriel, CA).

228

229 *RNA Extraction, cDNA Synthesis and qPCR Reactions*

230 Total RNA was extracted from coral holobiont tissue using Ribozol Reagent (Amresco, Solon, OH), and
231 digested with PerfeCTa DNase I (Quanta Biosciences, Gaithersberg, MD) to eliminate residual genomic

232 DNA. cDNA was synthesized using qScript cDNA Supermix (Quanta Biosciences, Gaithersberg, MD) and
233 expression analyses were subsequently performed by means of quantitative PCR (qPCR). Primers
234 specific for H2A.X and H4 histone genes were designed based on sequences retrieved from GenBank
235 databases for *Acropora cervicornis* and *A. formosa* (Table 1) using the Primer-BLAST software (Ye et al.,
236 2012). Histone H4 was used for normalization purposes. Primer efficiencies were calculated based on the
237 slope of calibration curves constructed using ten-fold dilution steps, according to the formula $E =$
238 $10^{-1/slope}$. The resulting gene expression profiles were subsequently examined in *A. cervicornis* RNA
239 samples by measuring SYBR green incorporation in a LightCycler 96 System (Roche, Mannheim,
240 Germany). cDNA amplifications were carried out in 45 cycles under the following conditions: Pre-
241 incubation at 95 °C for 10 min, denaturalization at 95 °C for 10 s, annealing at 60 °C for 10 s and
242 elongation at 72 °C for 10 s, including a final melting gradient up to 97 °C using a ramp of 4.4 °C x s⁻¹ to
243 confirm primer specificity. Each individual reaction was carried out in triplicate, including negative controls
244 (No Template Control, NTC; Non-Reverse Transcription Control, NRTC). Results were recorded as
245 normalized ratio values by the LightCycler 96 Software version 1.1 following the Pfaffl method (Pfaffl,
246 2001).

247

248 *gamma-H2A.X/H2A.X Ratio Analysis*

249 The quantification of histone H2A.X and its phosphorylated form (gamma-H2A.X) was implemented in
250 coral samples from different experimental treatments by using a commercial ELISA kit (Raybiotech,
251 Norcross, GA), providing a simultaneous semi-quantitative measure of the gamma-H2A.X/H2A.X ratio in a
252 single experiment. For that purpose, 10 mg of coral tissue from each of three samples per treatment per
253 time were solubilized in 500 µL of commercial lysis buffer and incubated on ice for 30 min. After
254 centrifugation (18,000 g for 10 min at 4 °C), 100 µL of each lysate were loaded by duplicate in anti-H2A.X
255 pre-coated microplate along with positive and negative controls provided in the kit, and samples were
256 incubated overnight at 4 °C. Subsequently, 100 µL of detection antibodies [anti-H2A.X (S139) or anti-pan-
257 H2A.X], HRP (Horseradish Peroxidase)-conjugated anti-rabbit IgG (against secondary antibodies) and
258 TMB One-Step Substrate Reagent were added to the plate following manufacturer's indications. The TMB

259 substrate was incubated for 30 min in the dark with shaking and 50 μ L of Stop Solution were added to
260 each well before reading absorbances in a ELx808IU microplate reader (Biotek, Winooski, VT) at 450 nm.

261

262 *DNA Extraction and DNA Methylation Analysis*

263 Genomic DNA was purified as described elsewhere and adapted to coral tissue in the present work.
264 Briefly, tissue homogenates was incubated at 50 °C for 2 h with CTAB lysis buffer (100 mM Tris, 20mM
265 EDTA, 1.2 M NaCl, 2% CTAB, pH 8.0) and proteinase K, completing DNA extraction following the phenol-
266 chloroform protocol (Sambrook & Russell, 2006). DNA methylation was quantified in genomic DNA
267 samples by measuring the amount of 5-methyl-Cytosines (5-mC), using the MethylFlash Global DNA
268 Methylation (5-mC) ELISA kit (Epigentek, Farmingdale, NY). Accordingly, three genomic DNA samples
269 per treatment/time were loaded in duplicate to ELISA plates, along with positive (polynucleotide with 50 %
270 of 5-mC) and negative controls (polynucleotide with 50% of unmethylated Cytosine), all with binding
271 solution. All samples were diluted to a final concentration of 9.645 ng/ μ L in NanoPure water,
272 corresponding to 77.12 ng of DNA in each well. Once binding was completed, 100 μ L of capture antibody,
273 detection antibody, developer solution and stop solution were sequentially added, performing intercalated
274 incubations and plate washes, following manufacturer indications. The absorbance (OD) resulting from the
275 colorimetric reaction was quantified at 450 nm in a ELx808IU microplate reader (Biotek, Winooski, VT).
276 Quantification of 5-methyl-Cytosine content (ng) was performed following the calculations suggested by
277 the manufacturer.

278

279 *Statistical Analyses*

280 All results are presented as mean values of replicate samples \pm standard error, unless indicated
281 otherwise. All statistical analyses were performed with respect to controls to separate the contributions of
282 the experimental variables. The statistical significance of the effect of blocks, treatments and exposure
283 time was evaluated by means of Two-Way ANOVA and One-Way ANOVA when required. This approach
284 was appropriate for the analysis of P content, histone H2A.X quantification, and DNA methylation after
285 transformation to natural logarithm. In all cases, data were confirmed to follow a normal distribution

286 (Shapiro-Wilk Test, $p > 0.05$), and variance homogeneity (Brown-Forsythe Test, $p > 0.05$). The analysis of
287 N content data (including N:P molar ratios) was done by means of a Two-Way PERMANOVA with
288 Euclidian distance using 9,999 permutations (Anderson, 2001). Although this is primarily a multivariate
289 method, it performs as a univariate test (equivalent to ANOVA) under the current experimental data
290 conditions, avoiding the assumption of normality (Anderson, 2017) and allowing for the analysis of
291 interactive effects (Doropoulos et al., 2014). PERMDISP was used to test for homogeneity of dispersion
292 (equivalent to homoscedasticity). Post-hoc Tukey-HSD tests and the Holm-Sidak method were used for
293 multiple comparisons when appropriate. All analyses were carried out using R 3.4.1 (R Core Team, 2017),
294 except the Two-Way PERMANOVA that was performed using PAST 3.18 (Hammer, Harper, & Ryan,
295 2001) and the PERMDISP analysis that was performed with Primer v6 (Clarke & Gorley, 2006)

296 **RESULTS**

297

298 *Nutrient Quantification and Thermal Monitoring During Experimental Treatments.*

299 The nutrient enrichment treatments implemented in the present work did not cause coral mortality, and no
300 bleaching or disease were evident during the experiment. In addition, it was determined that the studied
301 parameters were not influenced by the block design ($p > 0.05$, Table 2). N and P levels in the holobiont
302 displayed particularly low values (Fig. 2, Table 3), with %P around 0.4 and %N around 2.1 for all
303 treatments. Nonetheless, while neither N or P content displayed significant differences among treatments
304 (%P: $F_{(2, 34)} = 0.744$, $p = 0.483$; %N: $F_{(2, 34)} = 0.692$ $p = 0.427$), both parameters showed significant
305 changes during the span of the experiment, decreasing in the case of P content ($F_{(4, 34)} = 5.960$, $p =$
306 0.007 , Fig. 2A), and increasing in the case of N content ($F_{(4, 34)} = 10.527$, $p < 0.001$, Fig. 2B). As a result,
307 N:P molar ratios displayed a significant dependence with time ($F_{(4, 34)} = 13.62$, $p < 0.001$; Fig. 2C), as well
308 as a statistical dependence with the nutrient enrichment treatments assayed ($F_{(2, 34)} = 1.8245$ $p = 0.05$).
309 Interestingly, although tissue nutrient analyses were not very sensitive to the nutrient addition treatments
310 developed on the reef, results showed an antagonistic response of N and P through time, evidencing a
311 mild nutrient enrichment in holobiont tissues.

312

313 Given that the present experiment was directly developed in the reef, factors other than nutrient exposure
314 could be affecting the observed results, notably fluctuating thermal regimes. Consequently, temperature
315 data corresponding to the experimental site (long-term monitoring station, 4 Km away and at similar depth,
316 site 225, 25° 00.807', 80° 22.677') was subsequently analyzed to evaluate this possibility (Fig. 3). Results
317 revealed a temperature increase in the lower portion of the water column (up to 40 cm from the bottom)
318 from 28.39 ± 0.15 °C at the beginning of acclimatization period, to 30.52 ± 0.05 °C by the end of the
319 experiment. This represents a net increase of more than 2 °C during the exposure period, reaching the
320 bleaching threshold reported for *Acropora cervicornis* in the Florida Keys (30.5 °C; Manzello, Berkelmans,
321 & Hendee, 2007). Based on this observation, the effect of thermal stress was added to that of nutrient
322 stress, in order to better evaluate their combined effect on coral epigenetic responses.

323
324 *Changes in Symbiont Population Densities Across Nutrient Treatments.*
325 Symbiont density analyses revealed a significant increase in the symbiont populations of *A. cervicornis*
326 corals subject to nutrient enrichment treatments during the course of the present experiment (Table 4), as
327 compared with the constant density levels observed in corals subject to control conditions. Additionally,
328 the obtained results revealed that changes in symbiont densities were significantly influenced by the
329 specific nature of the nutrient treatments as follows: on one hand, corals exposed to N only enrichment
330 (treatment 1) displayed a twofold increase respect to control corals; on the other, a fourfold increase was
331 observed in corals exposed to N+P enrichment (treatment 2). Along with nutrient quantification analyses,
332 these results further support the efficiency of the nutrient exposures developed during the present work.

333
334 *Changes in Histone H2A.X Phosphorylation During Nutrient and Thermal Stress.*
335 Histones from *Acropora cervicornis* were extracted, isolated and purified for the first time in the present
336 work, including different fractions containing linker and core histones, as well as diverse histone-like
337 proteins present in the coral holobiont (Fig. 4A, B). In addition, H2A.X and its phosphorylated form
338 gamma-H2A.X were immunodetected using western blot analyses (Fig. 4C), validating the use of different
339 commercial antibodies for their detection in corals. The role of H2A.X during coral responses to nutrient
340 and thermal stress was studied at two different functional levels. First, coral H2A.X gene expression
341 patterns were analyzed using coral-specific qPCR primers specifically designed using *A. cervicornis* and
342 *A. formosa* sequences retrieved from GenBank databases as references (Table 1). The obtained results
343 revealed homogeneous gene expression levels across the different nutrient treatments during the first 24
344 h of exposure ($F_{(2, 9)} = 1.569$, $p = 0.265$, Fig. 5, Suppl. Fig. 1), suggesting that the main role of coral
345 H2A.X during responses to nutrient stress (temperature was not high enough to cause stress during the
346 first 24 h) does not take place at the transcriptional level.

347
348 The analysis of the epigenetic effects mediated by H2A.X was subsequently expanded to the post-
349 translational level, based on the well-established link between H2A.X phosphorylation and DNA damage

350 repair. For that purpose, gamma-H2A.X levels were quantified during coral exposure to different nutrient
351 treatments under increasing temperature, revealing significant differences between different treatments at
352 specific sampling times ($F_{(14, 40)} = 4.361, p < 0.001$) in spite of the high variability in the response of the
353 controls. These results can be interpreted as indicative of DNA damage occurring in higher rates under
354 enriched conditions, based on the stress marker nature of the gamma-H2A.X modification. Accordingly,
355 the observed response can be divided into three major stages (Fig. 6A): first, an early rapid response
356 consisting of a significant increase in gamma-H2A.X was observed during the first hour in corals subject to
357 both N and N + P treatments (Tukey-HSD test, $q = 16.264, p = 0.003$); second, a suspended gamma-
358 H2A.X response was observed in both treatments starting from hour 2 to day 7; and third, a late slow
359 response in gamma-H2A.X over a longer period of time that was observed after day 7. In this last period,
360 phosphorylation reached significantly different values in both enrichment treatments as follows: on one
361 hand, gamma-H2A.X became significantly greater than controls after a 20-day exposure to the N
362 treatment (Tukey-HSD test, $q = 4.734, p = 0.036$) and after a 35-day exposure to N + P treatment (Holm-
363 Sidak test, $t = 4.057, p < 0.001$); on the other, a reduction in gamma-H2A.X levels was observed in coral
364 fragments subject to N enrichment for more than 20 days, displaying significant differences respect to
365 controls upon reaching the 35-day mark (Holm-Sidak test, $t = 2.394, p = 0.021$).

366

367 *Changes in DNA Methylation During Nutrient and Thermal Stress.*

368 In addition to histone modifications, the role of DNA methylation during coral responses to nutrient stress
369 was analyzed in the present work to account for the potential interaction among multiple mechanisms
370 during epigenetic effects in response to environmental stress. In the present case, however, DNA
371 methylation analyses did not detect significant differences among different nutrient treatments ($F_{(2, 44)} =$
372 $2.505, p = 0.093$) or across different time points ($F_{(7, 44)} = 2.081, p = 0.066$) (Fig. 6B). Nonetheless, the
373 obtained results evidenced that the mean DNA methylation content in corals exposed to N enrichment
374 was twice as much as that experienced by control corals at hour 1, hour 2, day 7, day 27 and day 35. The
375 same was observed for corals exposed to N + P for day 27. Interestingly, this trend is similar (although no
376 significant correlation was observed) to that observed for gamma-H2A.X (Fig. 6A), including an initial rapid

377 response, followed by a suspended response and by a late slow response lasting until the end of the
378 experiment.

379 **DISCUSSION**

380 The present work constitutes one of the few pioneering efforts investigating the role of epigenetic
381 mechanisms during environmental responses in corals, more precisely to nutrient and thermal stress. In
382 doing so, this work also expands recent efforts combining the study of multiple epigenetic mechanisms
383 during environmental epigenetic responses in marine invertebrates, including histone variants (and their
384 modifications) and DNA methylation (Gonzalez-Romero et al., 2017; Li et al., 2018). The obtained results
385 constitute the first description of the histone variant H2A.X and its phosphorylated form, gamma-H2A.X, in
386 a stony coral species. Such findings, together with the histone diversity previously described in cnidarians
387 (Reddy, Ubhe, Sirwani, Lohokare, & Galande, 2017; Török et al., 2016) as well as in Symbiodiniaceae
388 dinoflagellates (Lin et al., 2015), unveil the potential contribution that chromatin-associated proteins
389 convey during epigenetic effects and inheritance linked to environmental epigenetic responses in this
390 group (Beal et al., 2018). Along with the study of DNA methylation levels, this work starts shaping our
391 knowledge about the potential interactions among different epigenetic mechanisms mediating
392 environmental responses, as well as their modulation by the combined action of different stressors (e.g.,
393 nutrients and temperature).

394

395 *Coral Nutrient Content Does Not Predict Environmental Nutrient Exposure*

396 Nutrient quantification analyses revealed a lack of correlation between nutrient content in the coral
397 holobiont and the expected environmental nutrient levels derived from the experimental exposures.
398 Nonetheless, a nutrient enrichment effect was evidenced by the N:P molar ratios estimated during
399 exposures (Fig. 2C), as well as by the increase in symbiont population densities across treatments (Table
400 4). Although nutrient content in water was not evaluated in this work, studies using the same enrichment
401 strategy in the same location and season, successfully enriched the water column by approximately 3 μM
402 N and 0.3 μM P in a 1 m radius around nutrient diffusers (Vega Thurber et al., 2014; Zaneveld et al.,
403 2016), supporting the success of the present experimental approach in locally elevating nutrient
404 concentrations available to experimental coral fragments. Indeed, it has been demonstrated that changes
405 in environmental nutrient concentrations are not necessarily linked to changes in tissue content (Achituv et

406 al., 1994; Godinot et al., 2009; Godinot, Ferrier-Pagès, Montagna, & Grover, 2011; G Muller-Parker,
407 Mccloskey, Hoegh-Guldberg, & Mcauley, 1994; Gisèle Muller-Parker et al., 1994). Accordingly, multiyear
408 nutrient enrichment experiment (including both N and P) demonstrated a strong nutrient stoichiometric
409 homeostasis and high constancy in coral holobiont tissue, regardless of elevated external nutrient levels,
410 and even in the presence of a significant increase in the ¹⁵N isotope in corals exposed to N enrichment
411 (Koop et al., 2001). Consequently, based on these observations as well as on the results obtained in the
412 present work, the lack of a cause-effect relationship between environmental nutrient enrichment and the
413 nutrient levels determined for coral tissues could be due to a rapid nutrient turnover in the holobiont.

414
415 On the other hand, nutrient content changed significantly with time and independently of nutrient
416 treatment, suggesting that other factors may be influencing nutrient content in coral tissue. Among the
417 different environmental parameters chiefly affecting coral fitness, it is well known that thermal stress can
418 modify coral nutrient uptake ratios (Ezzat et al., 2016; Godinot, Houlbrèque, et al., 2011), and regulate
419 phosphate transfer to symbiotic vacuoles (Miller & Yellowlees, 1989). The analysis of thermal regimes
420 during the present experiment revealed a progressive increase in water temperature in the area of study
421 (Fig. 3), potentially affecting the observed nutrient dynamics. Accordingly, among the different reports
422 addressing the effect of thermal stress on nutrient uptake ratios, at least one has described a sharp
423 increase in N uptake (with no change in P intake) in corals subject to mild thermal stress (29 °C, Godinot
424 et al., 2011), matching the observations described in the present work (Fig. 2A, B). On the other hand,
425 alternative studies have described an inverse pattern in coral species subject to severe thermal stress (>
426 30 °C, Ezzat et al., 2016; Godinot et al., 2011). Altogether, these results are illustrative of the complexity
427 of nutrient stress responses in corals, being possible that the thermal variation experienced by
428 experimental corals (28 - 30°C) contributed to the observed trends in nutrient contents.

429

430 *gamma-H2A.X Participates in Coral Epigenetic Responses to Nutrient and Thermal Stress*

431 Coral exposure to elevated nutrient levels can promote the rapid proliferation of symbionts, leading to a
432 potential increase in the production and export of ROS (Cunning & Baker, 2012; Ezzat et al., 2016;

433 Marubini & Davies, 1996; Nesa & Hidaka, 2009; Wiedenmann et al., 2012; Wooldridge, 2009), as well as
434 in DNA damage (Lesser, 2006). Under conditions of nutrient imbalance and/or thermal stress, such
435 deleterious effects are likely to be exacerbated by the damage experienced by the photosynthetic
436 machinery (Pogoreutz et al., 2017), as well as by the disruption of the symbiont's membrane composition
437 (Wiedenmann et al., 2012). Given the well-established role of histone H2A.X and its phosphorylated form
438 during the activation of DNA repair mechanisms in eukaryotes (Maréchal & Zou, 2013; Suarez-Ulloa et
439 al., 2015), the modifications observed in gamma-H2A.X/H2A.X levels are consistent with the role of this
440 mechanism mediating epigenetic effects during coral responses to nutrient stress, supporting the link
441 between exposure to nutrient/thermal stress and the presence of DNA damage.

442
443 The results from gene expression analyses indicate that the role played by H2A.X does not appear to take
444 place at a transcriptional level (Fig. 5, Suppl. Fig. 1). Only two other studies have evaluated H2A.X gene
445 expression in marine invertebrates, with contradictory results. On one hand, increased H2A.X.1 and
446 H2A.X.2 mRNA levels were found in *Hydra* exposed to the genotoxic agent bleomycin (Reddy et al.,
447 2017). On the other, no expression changes were observed on variants H2A.X, H2A.Z and macroH2A
448 during the exposure of the Eastern oyster *Crassostrea virginica* to marine toxins (Gonzalez-Romero et al.,
449 2017). Nonetheless, both studies reported increased gamma-H2A.X levels upon exposure to
450 environmental stress (Gonzalez-Romero et al., 2017; Reddy et al., 2017), supporting that the main
451 functional role of this variant during DNA repair is regulated at a post-translational level.

452
453 The results obtained in this work suggest a link between environmental (nutrient/thermal) stress and
454 histone H2A.X phosphorylation in corals. However, the observed patterns were complex. First, basal
455 gamma-H2A.X levels (gamma-H2A.X/H2A.X ratio > 3) in corals are higher than those found in other
456 eukaryotes including humans (Ji et al., 2017) and marine invertebrates (Gonzalez-Romero et al., 2017).
457 Such peculiarity can be interpreted in the context of the recurrent state of hyperoxia to which corals are
458 subject during the day, resulting from the photosynthetic activity of symbiotic algae (Kuhl, Cohen,
459 Dalsgaard, Jorgensen, & Revsbech, 1995; Shashar, Cohen, & Loya, 1993). This includes the production

460 of ROS (Dykens, Shick, Benoit, Buettner, & Winston, 1992), requiring frequent mitigation of the
461 subsequent oxidative damage in the coral holobiont (Richier, Furla, Plantivaux, Merle, & Allemand, 2005;
462 Roth, 2014). Precisely, such complex interaction between the coral host and the algal symbiont could also
463 explain the high variability observed for gamma-H2A.X/H2A.X ratios in controls. Second, the transition
464 from early rapid response, to suspended response, to late slow response periods in gamma-H2A.X levels
465 (Fig. 6A) agrees with coral acclimatory responses, necessary to activate molecular and physiological
466 mechanisms temporally restoring homeostasis until additional responses (usually more intense and
467 persistent than the previous) are required. Indeed, a similar dynamic response was observed during coral
468 exposure to thermal stress, involving two pulses in the expression of the heat shock protein *hsp70* linked
469 to acclimatization periods to different levels of stress (Gates & Edmunds, 1999). Similarly, Moya, Ganot,
470 Furla, & Sabourault (2012) observed a rapid and transient transcriptomic response to stress in the
471 anemone *Anemonia viridis*, followed by a second response after 5 or 21 days depending on the
472 combination of thermal stress and UV exposure. The obtained results are further supported by the
473 identification of pulse-like or transient responses in the expression and activity of stress proteins in coral
474 larvae (Rodriguez-Lanetty, Harii, & Hoegh-Guldberg, 2009; Voolstra et al., 2009), as well as in molluscs
475 exposed to thermal stress (Anestis, Lazou, Portner, & Michaelidis, 2007).

476
477 The final stage of the experiment was particularly interesting regarding histone H2A.X dynamics, as
478 gamma-H2A.X levels displayed significant differences with respect to controls but with different signs
479 depending on the nutrient treatment. Accordingly, gamma-H2A.X levels increased drastically in corals
480 exposed to N + P by day 35, which not only agrees with a prolonged exposure to nutrient stress, but also
481 with the increment in water temperature (more than 2 °C at this point). On the contrary, gamma-H2A.X
482 levels decreased significantly by day 35 in corals exposed to N only enrichment, which is a remarkable
483 observation considering that these individuals were also subject to thermal stress (and therefore require
484 as much DNA repair as possible). This is probably one of the most interesting results in the present work,
485 as it provides support for the hypothesis suggesting that N enrichment will promote P starvation in the
486 coral holobiont (Wiedenmann et al., 2012), hampering the phosphorylation of H2A.X and subsequent

487 activation of DNA repair mechanisms. In addition, P starvation has been proposed to increase thermally-
488 driven damage to photosystem II (Pogoreutz et al., 2017), as well as to limit the capacity of the thylakoid
489 membrane to contain ROS (Wiedenmann et al. 2012), further exacerbating DNA damage in cells where
490 DNA damage repair (by way of gamma-H2A.X formation) is already seriously impaired. On the other
491 hand, a higher level of H2A.X phosphorylation (indicative of DNA damage sensing and repair) will be
492 expected in corals exposed to N + P treatment after 35 days, as corroborated by the obtained results,
493 thanks to the presence of P as part of that treatment, therefore preventing the harmful effects of P
494 starvation.

495
496 Overall, the consequences of the impairment in H2A.X phosphorylation are enormous, as these will
497 directly affect the ability of the coral holobiont to activate DNA damage repair mechanisms (Albino et al.,
498 2009). Indeed, the alteration of this epigenetic mechanism could help explaining the synergistic effects of
499 nutrient imbalance and thermal stress on coral fitness, increasing bleaching and mortality (Ezzat et al.,
500 2016; Wooldridge, 2009). Similarly, these results also support the positive effect of P addition in order to
501 improve coral resilience to thermal stress (Ezzat et al., 2016).

502

503 *Global DNA Methylation*

504 Among the different epigenetic mechanisms known to date, DNA methylation is the best studied in marine
505 organisms (Beal et al., 2018; Eirin-Lopez & Putnam, 2019). In the present work, the analysis of global
506 DNA methylation did not detect significant differences among different nutrient treatments or across
507 different time points (Fig. 6B) . Such result is surprising, based on the multiple reports describing changes
508 in DNA methylation levels in marine organisms subject to different environmental stimuli (Beal et al., 2018;
509 Eirin-Lopez & Putnam, 2019). A possible explanation could involve the scale at which DNA methylation
510 was quantified in the present work. Accordingly, DNA methylation was estimated at a global genomic level
511 which provides little resolution, therefore, the marginal lack of significance observed could result from
512 limited replication. In addition, DNA methylation was quantified for the coral holobiont (including both the
513 coral host and the algal symbiont) introducing another potential source of variability affecting the results

514 obtained. In addition, the canceling effect that specific local modifications may have on each other cannot
515 be neglected. Lastly, both promoter and gene-body methylation (or the lack thereof) appear to contribute
516 to phenotypic plasticity in marine invertebrates (Eirin-Lopez & Putnam, 2019; Gavery & Roberts, 2013; Li
517 et al., 2018; Marsh & Pasqualone, 2014), making the study of this epigenetic mechanism extremely
518 complex in this group. An illustration of such complexity is exemplified by responses to stress involving an
519 increase in DNA methylation at specific genomic regions accompanied by demethylation at others,
520 resulting in a net genome-wide DNA methylation level similar to that present in controls (same number of
521 DNA methylation marks but at different genomic regions). Despite the limitations of the method, the
522 contribution of DNA methylation to coral stress responses is hinted by the trends observed, including
523 pulsed changes in DNA methylation mirroring those observed in the case of gamma-H2A.X/H2A.X ratios.
524 Since pulsed responses would facilitate immediate responses upon stress exposure, followed by the
525 activation of other complementary mechanisms mediating longer-term responses, it would not be
526 surprising if DNA methylation also follows such trend by regulating the expression of genes linked to other
527 mechanisms involved in the maintenance of genome integrity. Further analyses addressing changes in
528 DNA methylation variation at higher resolution (i.e., single nucleotide level) will be necessary in order to
529 clarify that aspect.

530

531 **CONCLUSIONS**

532 This work constitutes a pioneering effort describing coral epigenetic modifications during responses to
533 nutrient and thermal stress, including histone modifications and DNA methylation. The obtained results
534 support the presence of the specialized histone variant H2A.X and its phosphorylated form (gamma-
535 H2A.X) in stony corals. The relationship between gamma-H2A.X levels and coral exposure to stress
536 appears to be consistent with the role of this histone modification activating DNA repair responses. Such
537 function is further supported by the observed impairment of gamma-H2A.X formation after prolonged
538 exposure to N enrichment, underscoring the detrimental effects that P limitation bears on the epigenetic
539 mechanisms preserving coral genome integrity. Although the observed modifications in DNA methylation
540 during nutrient and thermal stress were not large enough to be statistically significant, the contribution of
541 this epigenetic mechanism to coral stress responses should not be disregarded based on: a) the global
542 nature of the DNA methylation estimations developed in this work; b) the similarity between the shape of
543 DNA methylation trends (2 major pulses during the experiment), and that of the gamma-H2A.X response
544 observed over the course of exposures; and c) the complexity of DNA methylation responses to
545 environmental stress described in marine invertebrates. Overall, this effort constitutes a first step toward
546 understanding the intricacies of the mechanisms regulating environmental epigenetic responses in marine
547 organisms. Further efforts will be required to bring this research to the next level, including genome-wide,
548 single-nucleotide resolution level studies to elucidate the regulatory relationships between different
549 epigenetic mechanisms and the genes involved in acclimatory and adaptive responses. Similarly, the
550 study of the interaction between the genome and the epigenome will help understand how population
551 diversity shapes epigenetic responses in marine populations, along with the implications for the
552 implementation of epigenetic selection methods. Although these goals will be even more challenging in
553 the specific case of corals (given the contribution of the symbiont genome and epigenome to the
554 phenotype of the holobiont) the potential benefits for improving restoration, management and conservation
555 of coral reef ecosystems worldwide clearly justifies that effort.

556

557 **ACKNOWLEDGMENTS**

558 This work was supported by grants from the National Science Foundation (Grant IOS 1810981 awarded to
559 JEL, and Grant HRD 1547798 awarded to Florida International University as part of the Centers for
560 Research Excellence in Science and Technology Program), and the Natural Science and Engineering
561 Research Council of Canada (Grant RGPIN-2017-04162 awarded to JA). We are thankful to the Coral
562 Restoration Foundation for providing the staghorn coral fragments used during this research, and to all the
563 volunteers at FIU's Environmental Epigenetics Lab who assisted during the early stages of this work. This
564 is contribution #104 from the Center for Coastal Oceans Research in the Institute for Water and the
565 Environment at Florida International University.

566

567 **Tables**

568 **Table 1.** qPCR primers used in histone gene expression analyses and species used as references for
569 their design.

Gene	Primer Name	Sequence (5' → 3')	Species
H2A.X	Ac-H2A.X-Fw	CTCAGGGAGGTGTTTTGCCA	<i>Acropora cervicornis</i>
	Ac-H2A.X-Rv	TGGCTTTGGGATGATTTCCCT	
H4	Af-H4-Fw	CCGGGCTCCCAGTAAAATGT	<i>Acropora formosa</i>
	Af-H4-Rv	TGTCGTATGGGGGAGGGATT	

570

571 **Table 2.** Two-way ANOVA analysis of the contribution of block design to the studied variables. %P and
572 %N represent percentage of dry weight for each element.

Variable	Source of Variation	df	F	p
%P	Block	3	0.574	0.636
	Treatment x Block	6	0.495	0.808
%N	Block	3	1.167	0.336
	Treatment x Block	6	0.407	0.869
gamma-H2A.X/H2A.X	Block	3	1.128	0.345
	Treatment x Block	6	0.183	0.833
DNA methylation	Block	3	1.920	0.156
	Treatment x Block	6	0.883	0.419

573

574 **Table 3.** Nutrient content in corals (holobiont) exposed to control (C), enriched nitrogen (N), and enriched
575 nitrogen and phosphorus (N+P) treatments. Values represent mean and standard deviation (in
576 parentheses) for all samples collected during a 4 week-long exposure (n=24). N:P and C:N represent
577 molar nitrogen:phosphorus and carbon:nitrogen ratios, respectively. %P, %N and %C represent
578 percentage of dry weight for each element.

Treatment	%P	%N	%C	N:P	C:N
C	0.382 (0.096)	2.136 (0.790)	15.592 (5.049)	3.011 (2.163)	6.350 (0.498)
N	0.420 (0.148)	2.135 (0.755)	15.298 (4.665)	2.875 (2.310)	6.286 (0.731)
N+P	0.404 (0.106)	2.116 (0.715)	15.791 (4.615)	2.493 (1.132)	6.480 (0.556)

579

580 **Table 4.** Mixed effects models analysis of modifications in symbiont population densities in *A. cervicornis*
581 during the course of the present experiment under control (C), enriched nitrogen (N), and enriched
582 nitrogen and phosphorus (N+P) treatments*.

Treatment	χ^2	Slope \pm SE	p
C	2.184	0.00034 \pm 0.00023	0.140
N	4.400	0.00084 \pm 0.00040	0.036
N+P	14.061	0.00100 \pm 0.00028	<0.001

583 * The slope represents the linear estimate of how the symbiont population changes through time (10^9 cell x hour⁻¹) in the different
584 treatments. See Statistical Methods in the Methods section of this work for additional details on symbiont density analyses.

585 **Legends to Figures**

586 **Fig. 1. A.** Field experiment site location in Pickles Reef, Upper Florida Keys, Key Largo, FL (25°00'05" N,
587 80°24'55"W). **B.** Nutrient exposure experiment design consisting of 12 blocks evenly distributed across the
588 study area (n = 4 blocks per treatment), randomly assigned to one of three treatment conditions: control
589 (C), Nitrogen enrichment (N), and Nitrogen and Phosphorous enrichment (N + P). **C.** Each coral fragment
590 was secured to PVC tubing set in a base of concrete using nylon cable ties, for a total of 12 fragments per
591 block.

592
593 **Fig. 2. A.** Nutrient content in tissue from staghorn coral fragments exposed to the different enrichment
594 treatments implemented in the present work. **A.** Phosphorus tissue content in coral fragments expressed
595 as percent of dry mass of reactive phosphate; **B.** Nitrogen tissue content in coral fragments expressed as
596 percent of dry mass; **C.** N:P molar ratio. Exposure times are defined as: T1, hour 1 to day 3; T2, day 3 to
597 day 20; and T3, day 20 to day 35.

598
599 **Fig. 3.** Hourly water column temperatures in the Florida Keys National Marine Sanctuary, site 225, for the
600 year 2015. The blue line represents the mean value for the temperature registered in this station for the
601 year. The periods corresponding to the different stages of the experiment are indicated in green
602 (acclimatization of coral fragments) and red (exposure of coral fragments to nutrient enrichment
603 treatments).

604
605 **Fig. 4. A.** Purification profile of acid-extracted staghorn coral histones across an acetonitrile gradient
606 (ACN) using HPLC. The analyzed histone fractions are indicated by numbers 1-12. **B.** SDS-PAGE
607 separation of HPLC histone fractions 1-12 revealing linker and core histones, as well as diverse histone-
608 like proteins present in the coral holobiont. **C.** Western blot immunodetection of histone variant H2A.X and
609 its phosphorylated form (gamma-H2A.X) to validate antibody specificity (above) and of HCl-extracted
610 histones from *A. cervicornis* (below) using commercial antibodies H2A.X.ab (Abcam), γ -H2A.X ab
611 (Abcam), H2A.Xry (RayBiotech) and γ -H2A.Xry (RayBiotech). ACN, acetonitrile; CM, chicken marker; M:
612 molecular weight marker; CR, coral tissue extraction; SS, starting sample.

613
614 **Fig. 5.** Histone H2A.X gene expression levels in staghorn coral during the first 24 hours of exposure to
615 different nutrient treatments. Plots represent mean normalized ratios in relation to the study calibrator
616 (Histone H4) \pm SE (n=2).

617
618 **Fig. 6. A.** Characterization of histone H2A.X phosphorylation levels in staghorn coral fragments across
619 different nutrient treatments, estimated as the ratio between phosphorylated H2A.X (gamma-H2A.X) and
620 its non-modified form (H2A.X). Each plot represents mean \pm SE (n = 3). The level of significance of the
621 post-hoc Holm-Sidak test is indicated as * $p < 0.05$, ** $p < 0.01$. The response was divided into three parts:
622 early rapid response (hour 1), suspended response (hour 2 - day 7), and late slow response (after day 7).
623 **B.** Characterization of global DNA methylation levels in staghorn coral fragments across different nutrient
624 treatments, estimated as total mass of methylated (5-methyl-Cytosine) DNA. Each plot represents mean \pm
625 SE (n = 3, biological replicates). The response was divided in three parts mirroring gamma-H2A.X, defined
626 as: early rapid response (hour 1 - 2), suspended response (hour 2 - day 14), and late slow response until
627 the end of the experiment (after day 14).

628

629 **Suppl. Fig. 1.** Principal coordinate analysis (PCoA) of histone H2A.X gene expression values revealing
630 homogeneous gene expression levels across different nutrient treatments during the first 24 h of
631 exposure. H1, 1 h exposure; H5, 5 h exposure; H24, 24 h exposure. C, control; N, N only exposure
632 (treatment 1); N-P, N+P exposure (treatment 2).

633

634 REFERENCES

- 635 Achituv, Y., Ben-Zion, M., & Mizrahi, L. (1994). Carbohydrate, lipid, and protein composition of
636 zooxanthellae and animal fractions of the coral *Pocillopora damicornis* exposed to ammonium
637 enrichment. *Pacific Science*, 48(3), 224–233. Retrieved from
638 <http://scholarspace.manoa.hawaii.edu/bitstream/10125/2231/1/v48n3-224-233.pdf>
- 639 Anderson, M. J. (2001). A new method for non-parametric multivariate analysis of variance. *Austral Ecol*,
640 26(September), 32–46. <https://doi.org/10.1111/j.1442-9993.2001.01070.pp.x>
- 641 Anestis, A., Lazou, A., Portner, H. O., & Michaelidis, B. (2007). Behavioral, metabolic, and molecular
642 stress responses of marine bivalve *Mytilus galloprovincialis* during long-term acclimation at
643 increasing ambient temperature. *AJP: Regulatory, Integrative and Comparative Physiology*, 293(2),
644 R911–R921. <https://doi.org/10.1152/ajpregu.00124.2007>
- 645 Ayre, D. J., & Hughes, T. P. (2000). Genotypic diversity and gene flow in brooding and spawning corals
646 along the great barrier reef, Australia. *Evolution*, 54(5), 1590–1605. <https://doi.org/10.1111/j.0014-3820.2000.tb00704.x>
- 648 Ayre, D. J., & Hughes, T. P. (2004). Climate change, genotypic diversity and gene flow in reef-building
649 corals. *Ecology Letters*, 7(4), 273–278. <https://doi.org/10.1111/j.1461-0248.2004.00585.x>
- 650 Barshis, D. J., Ladner, J. T., Oliver, T. A., Seneca, F. O., Traylor-Knowles, N., & Palumbi, S. R. (2013).
651 Genomic basis for coral resilience to climate change. *Proceedings of the National Academy of*
652 *Sciences*, 110(4), 1387–1392. <https://doi.org/10.1073/pnas.1210224110>
- 653 Baruch, R., Avishai, N., & Rabinowitz, C. (2005). UV incites diverse levels of DNA breaks in different
654 cellular compartments of a branching coral species. *The Journal of Experimental Biology*, 208(Pt 5),
655 843–848. <https://doi.org/10.1242/jeb.01496>
- 656 Beal, A., Rodriguez-Casariago, J., Rivera-Casas, C., Suarez-Ulloa, V., & Eirín-López, J. M. (2018).
657 Environmental epigenomics and its applications in marine organisms. In M. Oleksiak & O. Rajora
658 (Eds.), *Population Genomics: Marine Organisms* (p. in press). Springer Nature.
- 659 Brown, B. E. (1997). Coral bleaching: causes and consequences. *Coral Reefs*, 16(0), 129–138.
660 <https://doi.org/10.1007/s003380050249>
- 661 Bruno, J. F., & Edmunds, P. J. (1997). Clonal variation for phenotypic plasticity in the coral *Madracis*
662 *mirabilis*. *Ecology*, 78(7), 2177–2190. [https://doi.org/10.1890/0012-9658\(1997\)078\[2177:cvfppi\]2.0.co;2](https://doi.org/10.1890/0012-9658(1997)078[2177:cvfppi]2.0.co;2)
- 664 Clarke, K. R., & Gorley, R. N. (2006). *PRIMER v6: User Manual/Tutorial*. Plymouth: PRIMER-E.
- 665 Cunning, R., & Baker, A. C. (2012). Excess algal symbionts increase the susceptibility of reef corals to
666 bleaching. *Nature Climate Change*, 3(3), 259–262. Retrieved from
667 <http://www.nature.com/doifinder/10.1038/nclimate1711>
- 668 D'Angelo, C., & Wiedenmann, J. (2014). Impacts of nutrient enrichment on coral reefs: New perspectives
669 and implications for coastal management and reef survival. *Current Opinion in Environmental*
670 *Sustainability*. <https://doi.org/10.1016/j.cosust.2013.11.029>
- 671 Deans, C., & Maggert, K. A. (2015). What Do You Mean, “Epigenetic”? *Genetics*, 199(4), 775–792.
672 <https://doi.org/10.1534/genetics.114.173492>
- 673 Dimond, J. L., & Roberts, S. B. (2016). Germline DNA methylation in reef corals: Patterns and potential
674 roles in response to environmental change. *Molecular Ecology*, 25(8), 1895–1904.
675 <https://doi.org/10.1111/mec.13414>
- 676 Dixon, G. B., Bay, L. K., & Matz, M. V. (2014). Bimodal signatures of germline methylation are linked with
677 gene expression plasticity in the coral *Acropora millepora*. *BMC Genomics*, 15(1), 1109.
678 <https://doi.org/10.1186/1471-2164-15-1109>
- 679 Doropoulos, C., Roff, G., Zupan, M., Nestor, V., Isechal, A. L., & Mumby, P. J. (2014). Reef-scale failure of
680 coral settlement following typhoon disturbance and macroalgal bloom in Palau, Western Pacific.
681 *Coral Reefs*, 33(3), 613–623. <https://doi.org/10.1007/s00338-014-1149-y>
- 682 Downs, C. A., Fauth, J. E., Halas, J. C., Dustan, P., Bemiss, J., & Woodley, C. M. (2002). Oxidative stress
683 and seasonal coral bleaching. *Free Radical Biology and Medicine*, 33(4), 533–543.
684 [https://doi.org/10.1016/S0891-5849\(02\)00907-3](https://doi.org/10.1016/S0891-5849(02)00907-3)
- 685 Dunn, J. G., Sammarco, P. W., & LaFleur, G. (2012). Effects of phosphate on growth and skeletal density
686 in the scleractinian coral *Acropora muricata*: A controlled experimental approach. *Journal of*

687 *Experimental Marine Biology and Ecology*, 411, 34–44. <https://doi.org/10.1016/j.jembe.2011.10.013>

688 Dykens, J. A., Shick, J. M., Benoit, C., Buettner, G. R., & Winston, G. W. (1992). Oxygen Radical
689 Production in the Sea Anemone *Anthopleura Elegantissima* and its Endosymbiotic Algae. *Journal of*
690 *Experimental Biology*, 168(1), 219–241. Retrieved from
691 <https://pdfs.semanticscholar.org/83a1/e3b392cbc36764e0778d876bd212fd04af4c.pdf>

692 Eirin-Lopez, J. M., & Putnam, H. M. (2019). Marine Environmental Epigenetics. *Annual Review of Marine*
693 *Science*, 11(1), annurev-marine-010318-095114. [https://doi.org/10.1146/annurev-marine-010318-](https://doi.org/10.1146/annurev-marine-010318-095114)
694 095114

695 Ezzat, L., Maguer, J.-F., Grover, R., & Ferrier-Pagès, C. (2016). Limited phosphorus availability is the
696 Achilles heel of tropical reef corals in a warming ocean. *Scientific Reports*, 6(August), 31768.
697 <https://doi.org/10.1038/srep31768>

698 Fabricius, K. E. (2005). Effects of terrestrial runoff on the ecology of corals and coral reefs: review and
699 synthesis. *Marine Pollution Bulletin*, 50, 125–146.

700 Fourqurean, J. W., Zieman, J. C., & Powell, G. V. N. (1992). Phosphorus limitation of primary production
701 in Florida Bay: Evidence from C: N: P ratios of the dominant seagrass *Thalassia testudinum*.
702 *Limnology and Oceanography*, 37(1), 162–171. <https://doi.org/10.4319/lo.1992.37.1.0162>

703 Gates, R. D., & Edmunds, P. J. (1999). The Physiological Mechanisms of Acclimatization in Tropical Reef
704 Corals. *American Zoologist*, 39(1), 30–43. <https://doi.org/10.1093/icb/39.1.30>

705 Gavery, M. R., & Roberts, S. B. (2013). Predominant intragenic methylation is associated with gene
706 expression characteristics in a bivalve mollusc. *PeerJ*, 1, e215. <https://doi.org/10.7717/peerj.215>

707 Godinot, C., Ferrier-Pagès, C., & Grover, R. (2009). Control of phosphate uptake by zooxanthellae and
708 host cells in the scleractinian coral *Stylophora pistillata*. *Limnology and Oceanography*, 54(5), 1627–
709 1633. <https://doi.org/10.4319/lo.2009.54.5.1627>

710 Godinot, C., Ferrier-Pagès, C., Montagna, P., & Grover, R. (2011). Tissue and skeletal changes in the
711 scleractinian coral *Stylophora pistillata* Esper 1797 under phosphate enrichment. *Journal of*
712 *Experimental Marine Biology and Ecology*, 409(1–2), 200–207.
713 <https://doi.org/10.1016/j.jembe.2011.08.022>

714 Godinot, C., Houlbrèque, F., Grover, R., & Ferrier-Pagès, C. (2011). Coral uptake of inorganic phosphorus
715 and nitrogen negatively affected by simultaneous changes in temperature and pH. *PLoS ONE*, 6(9),
716 e25024. <https://doi.org/10.1371/journal.pone.0025024>

717 González-Romero, R., Rivera-Casas, C., Fernández-Tajes, J., Ausió, J., Méndez, J., & Eirín-López, J. M.
718 (2012). Chromatin specialization in bivalve molluscs: A leap forward for the evaluation of Okadaic
719 Acid genotoxicity in the marine environment. *Comparative Biochemistry and Physiology - C*
720 *Toxicology and Pharmacology*, 155(2), 175–181. <https://doi.org/10.1016/j.cbpc.2011.09.003>

721 Gonzalez-Romero, R., Suarez-Ulloa, V., Rodriguez-Casariago, J., Garcia-Souto, D., Diaz, G., Smith, A.,
722 ... Eirin-Lopez, J. M. (2017). Effects of Florida Red Tides on histone variant expression and DNA
723 methylation in the Eastern oyster *Crassostrea virginica*. *Aquatic Toxicology*, 186, 196–204.
724 <https://doi.org/10.1016/j.aquatox.2017.03.006>

725 Hammer, Ø., Harper, D. A. T., & Ryan, P. D. (2001). PAST: Paleontological Statistics Software Package
726 for Education and Data Analysis. *Palaeontologia Electronica*, 4(1), 9pp. Retrieved from
727 https://www.uv.es/~pardomv/pe/2001_1/past/pastprog/past

728 Heck, K. L., Pennock, J. R., Valentine, J. F., Coen, L. D., & Sklenar, S. A. (2000). Effects of nutrient
729 enrichment and small predator density on seagrass ecosystems: An experimental assessment.
730 *Limnology and Oceanography*, 45(5), 1041–1057. <https://doi.org/10.4319/lo.2000.45.5.1041>

731 Hoegh-Guldberg, O., Mumby, J., Hooten, J., Steneck, S., Greenfield, P., Gomes, E., ... Hatzitolos, E.
732 (2007). Coral reefs under rapid climate change and ocean acidification. *Science*, 318(5857), 1737.

733 Hughes, T. P., Kerry, J. T., Álvarez-Noriega, M., Álvarez-Romero, J. G., Anderson, K. D., Baird, A. H., ...
734 Wilson, S. K. (2017). Global warming and recurrent mass bleaching of corals. *Nature*, 543(7645).
735 <https://doi.org/10.1038/nature21707>

736 Ji, J., Zhang, Y., Redon, C. E., Reinhold, W. C., Chen, A. P., Fogli, L. K., ... Bonner, W. M. (2017).
737 Phosphorylated fraction of H2AX as a measurement for DNA damage in cancer cells and potential
738 applications of a novel assay. *PLoS ONE*, 12(2), e0171582.
739 <https://doi.org/10.1371/journal.pone.0171582>

740 Koop, K., Booth, D., Broadbent, A., Brodie, J., Bucher, D., Capone, D., ... Yellowlees, D. (2001).

741 ENCORE: The effect of nutrient enrichment on coral reefs. Synthesis of results and conclusions.
742 *Marine Pollution Bulletin*, 42(2), 91–120. [https://doi.org/10.1016/S0025-326X\(00\)00181-8](https://doi.org/10.1016/S0025-326X(00)00181-8)

743 Kuhl, M., Cohen, Y., Dalsgaard, T., Jorgensen, B. B., & Revsbech, N. P. (1995). Microenvironment and
744 photosynthesis of zooxanthellae in scleractinian corals studied with microsensors for O₂, pH and
745 light. *Marine Ecology Progress Series*, 117(1–3), 159–177. <https://doi.org/10.3354/meps117159>

746 Leal, M. C., Hoadley, K., Pettay, D. T., Grajales, A., Calado, R., & Warner, M. E. (2015). Symbiont type
747 influences trophic plasticity of a model cnidarian-dinoflagellate symbiosis. *Journal of Experimental*
748 *Biology*, 218(6), 858–863. <https://doi.org/10.1242/jeb.115519>

749 Lesser, M. P. (2006). Oxidative Stress in Marine Environments: Biochemistry and Physiological Ecology.
750 *Annual Review of Physiology*, 68(1), 253–278.
751 <https://doi.org/10.1146/annurev.physiol.68.040104.110001>

752 Li, Y., Liew, Y. J., Cui, G., Cziesielski, M. J., Zahran, N., Michell, C. T., ... Aranda, M. (2018). DNA
753 methylation regulates transcriptional homeostasis of algal endosymbiosis in the coral model *Aiptasia*.
754 *Science Advances*, 4(8), eaat2142. <https://doi.org/10.1126/sciadv.aat2142>

755 Liew, Y. J., Zoccola, D., Li, Y., Tambutte, E., Venn, A. A., Michell, C. T., ... Aranda, M. (2018).
756 Epigenome-associated phenotypic acclimatization to ocean acidification in a reef-building coral.
757 *Science Advances*, 4(6), eaar8028. <https://doi.org/10.1126/sciadv.aar8028>

758 Lin, S., Cheng, S., Song, B., Zhong, X., Lin, X., Li, W., ... Morse, D. (2015). The Symbiodinium kawagutii
759 genome illuminates dinoflagellate gene expression and coral symbiosis. *Science*, 350(6261), 691–
760 694. <https://doi.org/10.1126/science.aad0408>

761 Loya, Y., Lubinevsky, H., Rosenfeld, M., & Kramarsky-Winter, E. (2004). Nutrient enrichment caused by in
762 situ fish farms at Eilat, Red Sea is detrimental to coral reproduction. *Marine Pollution Bulletin*, 49(4),
763 344–353. <https://doi.org/10.1016/j.marpolbul.2004.06.011>

764 Manzello, D. P., Berkelmans, R., & Hendee, J. C. (2007). Coral bleaching indices and thresholds for the
765 Florida Reef Tract, Bahamas, and St. Croix, US Virgin Islands. *Marine Pollution Bulletin*, 54(12),
766 1923–1931. <https://doi.org/10.1016/j.marpolbul.2007.08.009>

767 Maréchal, A., & Zou, L. (2013). DNA Damage Sensing by the ATM and ATR Kinases. *Cold Spring Harb*
768 *Perspect Biol*, 5, a012716. <https://doi.org/10.1101/cshperspect.a012716>

769 Marsh, A. G., Hoadley, K. D., & Warner, M. E. (2016). Distribution of CpG motifs in upstream gene
770 domains in a reef coral and sea anemone: Implications for epigenetics in cnidarians. *PLoS ONE*,
771 11(3), e0150840. <https://doi.org/10.1371/journal.pone.0150840>

772 Marsh, A. G., & Pasqualone, A. A. (2014). DNA methylation and temperature stress in an Antarctic
773 polychaete, *Spiophanes tcherniai*. *Frontiers in Physiology*, 5, 173.
774 <https://doi.org/10.3389/fphys.2014.00173>

775 Marubini, F., & Davies, P. S. (1996). Nitrate increases zooxanthellae population density and reduces
776 skeletogenesis in corals. *Marine Biology*, 127(2), 319–328. <https://doi.org/10.1007/BF00942117>

777 McGinty, E. S., Pieczonka, J., & Mydlarz, L. D. (2012). Variations in reactive oxygen release and
778 antioxidant activity in multiple Symbiodinium types in response to elevated temperature. *Microbial*
779 *Ecology*, 64(4), 1000–1007. <https://doi.org/10.1007/s00248-012-0085-z>

780 Miller, D. J., & Yellowlees, D. (1989). Inorganic Nitrogen Uptake by Symbiotic Marine Cnidarians: A
781 Critical Review. *Proceedings of the Royal Society B: Biological Sciences*, 237(1286), 109–125.
782 <https://doi.org/10.1098/rspb.1989.0040>

783 MOYA, A., GANOT, P., FURLA, P., & SABOURAULT, C. (2012). The transcriptomic response to thermal
784 stress is immediate, transient and potentiated by ultraviolet radiation in the sea anemone *Anemonia*
785 *viridis*. *Molecular Ecology*, 21(5), 1158–1174. <https://doi.org/10.1111/j.1365-294X.2012.05458.x>

786 Muller-Parker, G., Cook, C. B., & D'Elia, C. F. (1994). Elemental composition of the coral *Pocillopora*
787 *damicornis* exposed to elevated seawater ammonium. *Pacific Science*, 48(3), 234–246.

788 Muller-Parker, G., McCloskey, L. R., Hoegh-Guldberg, O., & McAuley, P. J. (1994). Effect of Ammonium
789 Enrichment on Animal and Algal Biomass of the Coral *Pocillopora damicornis*. *Pacific Science*,
790 48(3), 273–283. Retrieved from [http://hl-128-171-57-
791 22.library.manoa.hawaii.edu/bitstream/10125/2236/1/v48n3-273-283.pdf](http://hl-128-171-57-22.library.manoa.hawaii.edu/bitstream/10125/2236/1/v48n3-273-283.pdf)

792 Nesa, B., Baird, A. H., Harii, S., Yakovleva, I., & Hidaka, M. (2012). Algal Symbionts Increase DNA
793 Damage in Coral Planulae Exposed to Sunlight. *Zoological Studies*, 51(1), 12–17. Retrieved from
794 <http://zoolstud.sinica.edu.tw/Journals/51.1/12.pdf>

795 Nesa, B., & Hidaka, M. (2009). High zooxanthella density shortens the survival time of coral cell
796 aggregates under thermal stress. *Journal of Experimental Marine Biology and Ecology*, 368(1), 81–
797 87. <https://doi.org/10.1016/j.jembe.2008.10.018>

798 Nielsen, D. A., Petrou, K., & Gates, R. D. (2018). Coral bleaching from a single cell perspective. *The ISME*
799 *Journal*. <https://doi.org/10.1038/s41396-018-0080-6>

800 Palumbi, S. R., Barshis, D. J., Taylor-Knowles Nikki, & Bay, R. A. (2014). Mechanisms of reef coral
801 resistance to future climate change. *Science*, 344(6186), 895–898.
802 <https://doi.org/10.1126/science.1251336>

803 Pandolfi, J. M., Bradbury, R., Sala, E., Hughes, T. P., Bjorndal, K. A., Cooke, R., ... Jackson, J. B. C.
804 (2003). Climate change, human impacts, and the resilience of coral reefs. *Science*, 301(5635), 955–
805 958. <https://doi.org/10.1126/science.1085046>

806 Pfaffl, M. W. (2001). A new mathematical model for relative quantification in real-time RT-PCR. *Nucleic*
807 *Acids Research*, 29(9), e45. <https://doi.org/10.1093/nar/29.9.e45>

808 Pogoreutz, C., Rädercker, N., Cárdenas, A., Gärdes, A., Voolstra, C. R., & Wild, C. (2017). Sugar
809 enrichment provides evidence for a role of nitrogen fixation in coral bleaching. *Global Change*
810 *Biology*, 23(9), 3838–3848. <https://doi.org/10.1111/gcb.13695>

811 Putnam, H. M., Davidson, J., & Gates, R. D. (2016). Ocean acidification influences DNA methylation and
812 phenotypic plasticity in environmentally susceptible corals. *Evolutionary Applications*, 56, E177–
813 E177. <https://doi.org/10.1111/eva.12408>

814 Reddy, P. C., Ubhe, S., Sirwani, N., Lohokare, R., & Galande, S. (2017). Title: Rapid divergence of
815 histones in Hydrozoa (Cnidaria) and evolution of a novel histone involved in DNA damage response
816 in hydra. *Zoology*. <https://doi.org/10.1016/j.zool.2017.06.005>

817 Richier, S., Furla, P., Plantivaux, A., Merle, P., & Allemand, D. (2005). Symbiosis-induced adaptation to
818 oxidative stress. *Journal of Experimental Biology*, 208(2), 277–285. <https://doi.org/10.1242/jeb.01368>

819 Rivera-Casas, C., Gonzalez-Romero, R., Garduño, R. A., Cheema, M. S., Ausio, J., & Eirin-Lopez, J. M.
820 (2017). Molecular and biochemical methods useful for the epigenetic characterization of chromatin-
821 associated proteins in bivalve molluscs. *Frontiers in Physiology*, 8(AUG), 490.
822 <https://doi.org/10.3389/fphys.2017.00490>

823 Rodriguez-Lanetty, M., Harii, S., & Hoegh-Guldberg, O. (2009). Early molecular responses of coral larvae
824 to hyperthermal stress. *Molecular Ecology*, 18(24), 5101–5114. <https://doi.org/10.1111/j.1365-294X.2009.04419.x>

826 Roth, M. S. (2014). The engine of the reef: Photobiology of the coral-algal symbiosis. *Frontiers in*
827 *Microbiology*. <https://doi.org/10.3389/fmicb.2014.00422>

828 Sambrook, J., & Russell, D. W. (2006). Purification of nucleic acids by extraction with phenol:chloroform.
829 *Cold Spring Harb Protoc*, 2006(1). <https://doi.org/10.1101/pdb.prot4455>

830 Saragosti, E., Tchernov, D., Katsir, A., & Shaked, Y. (2010). Extracellular production and degradation of
831 superoxide in the coral *Stylophora pistillata* and cultured symbiodinium. *PLoS ONE*, 5(9), 1–10.
832 <https://doi.org/10.1371/journal.pone.0012508>

833 Schübeler, D. (2015, January 15). Function and information content of DNA methylation. *Nature*. Nature
834 Publishing Group. <https://doi.org/10.1038/nature14192>

835 Shantz, A. A., & Burkepile, D. E. (2014). Context-dependent effects of nutrient loading on the coral-algal
836 mutualism. *Ecology*, 95(7), 1995–2005. <https://doi.org/10.1890/13-1407.1>

837 Shashar, N., Cohen, Y., & Loya, Y. (1993). Extreme Diel Fluctuations of Oxygen in Diffusive Boundary
838 Layers Surrounding Stony Corals. *Biol. Bull*, 185, 455–461. Retrieved from
839 <http://www.journals.uchicago.edu/t-and-c>

840 Silverstein, R. N., Cunning, R., & Baker, A. C. (2015). Change in algal symbiont communities after
841 bleaching, not prior heat exposure, increases heat tolerance of reef corals. *Global Change Biology*,
842 21(1), 236–249. <https://doi.org/10.1111/gcb.12706>

843 Silverstein, R. N., Cunning, R., & Baker, A. C. (2017). Tenacious D: Symbiodinium in clade D remain in
844 reef corals at both high and low temperature extremes despite impairment. *The Journal of*
845 *Experimental Biology*, 220, 1192–1196. <https://doi.org/10.1242/jeb.148239>

846 Solórzano, L., & Sharp, J. H. (1980). Determination of total dissolved phosphorus and particulate
847 phosphorus in natural waters. *Limnology and Oceanography*, 25(4), 754–758.
848 <https://doi.org/10.4319/lo.1980.25.4.0754>

- 849 Sotka, E. E., & Hay, M. E. (2009). Effects of herbivores, nutrient enrichment, and their interactions on
850 macroalgal proliferation and coral growth. *Coral Reefs*, 28(3), 555–568.
851 <https://doi.org/10.1007/s00338-009-0529-1>
- 852 Souter, P. (2010). Hidden genetic diversity in a key model species of coral. *Marine Biology*, 157(4), 875–
853 885. <https://doi.org/10.1007/s00227-009-1370-3>
- 854 Stillman, J. H., & Armstrong, E. (2015, March 1). Genomics are transforming our understanding of
855 responses to climate change. *BioScience*. Oxford University Press.
856 <https://doi.org/10.1093/biosci/biu219>
- 857 Suarez-Ulloa, V., Gonzalez-Romero, R., & Eirin-Lopez, J. M. (2015). Environmental epigenetics: A
858 promising venue for developing next-generation pollution biomonitoring tools in marine invertebrates.
859 *Marine Pollution Bulletin*, 98(1–2), 5–13. <https://doi.org/10.1016/j.marpolbul.2015.06.020>
- 860 Török, A., Schiffer, P. H., Schnitzler, C. E., Ford, K., Mullikin, J. C., Baxevanis, A. D., ... Gornik, S. G.
861 (2016). The cnidarian *Hydractinia echinata* employs canonical and highly adapted histones to pack
862 its DNA. *Epigenetics & Chromatin*, 9(1), 36. <https://doi.org/10.1186/s13072-016-0085-1>
- 863 van Oppen, M. J. H., Oliver, J. K., Putnam, H. M., & Gates, R. D. (2015). Building coral reef resilience
864 through assisted evolution. *Proceedings of the National Academy of Sciences*, 112(8), 1–7.
865 <https://doi.org/10.1073/pnas.1422301112>
- 866 Vega Thurber, R. L., Burkepile, D. E., Fuchs, C., Shantz, A. A., McMinds, R., & Zaneveld, J. R. (2014).
867 Chronic nutrient enrichment increases prevalence and severity of coral disease and bleaching.
868 *Global Change Biology*, 20(2), 544–554. <https://doi.org/10.1111/gcb.12450>
- 869 Voolstra, C. R., Schnetzer, J., Peshkin, L., Randall, C. J., Szmant, A. M., & Medina, M. (2009). Effects of
870 temperature on gene expression in embryos of the coral *Montastraea faveolata*. *BMC Genomics*,
871 10(1), 627. <https://doi.org/10.1186/1471-2164-10-627>
- 872 Wagner, D., Kramer, P., & van Woesik, R. (2010). Species composition, habitat, and water quality
873 influence coral bleaching in southern Florida. *Marine Ecology Progress Series*, 408, 65–78.
874 <https://doi.org/10.3354/meps08584>
- 875 Wiedenmann, J., D'angelo, C., Smith, E. G., Hunt, A. N., Legiret, F.-E., Postle, A. D., & Achterberg, E. P.
876 (2012). Nutrient enrichment can increase the susceptibility of reef corals to bleaching. *Nature*
877 *Climate Change*, 3(2), 160–164. Retrieved from
878 <http://www.nature.com/doi/10.1038/nclimate1661>
- 879 Wooldridge, S. A. (2009). Water quality and coral bleaching thresholds: Formalising the linkage for the
880 inshore reefs of the Great Barrier Reef, Australia. *Marine Pollution Bulletin*, 58(5), 745–751.
881 <https://doi.org/10.1016/j.marpolbul.2008.12.013>
- 882 Yakovleva, I. M., Baird, A. H., Yamamoto, H. H., Bhagooli, R., Nonaka, M., & Hidaka, M. (2009). Algal
883 symbionts increase oxidative damage and death in coral larvae at high temperatures. *Marine*
884 *Ecology Progress Series*, 378, 105–112. <https://doi.org/10.3354/meps07857>
- 885 Ye, J., Coulouris, G., Zaretskaya, I., Cutcutache, I., Rozen, S., & Madden, T. L. (2012). Primer-BLAST: A
886 tool to design target-specific primers for polymerase chain reaction. *BMC Bioinformatics*, 13(1), 134.
887 <https://doi.org/10.1186/1471-2105-13-134>
- 888 Zaneveld, J. R., Burkepile, D. E., Shantz, A. A., Pritchard, C. E., McMinds, R., Payet, J. P., ... Vega
889 Thurber, R. L. (2016). Overfishing and nutrient pollution interact with temperature to disrupt coral
890 reefs down to microbial scales. *Nature Communications*, (May), 1–12.
891 <https://doi.org/10.1038/ncomms11833>
- 892 Zaneveld, J. R., McMinds, R., & Thurber, R. V. (2017). Stress and stability: Applying the Anna Karenina
893 principle to animal microbiomes. *Nature Microbiology*. <https://doi.org/10.1038/nmicrobiol.2017.121>
- 894

895

896 **Data Accessibility Statement**

897 Data corresponding to sampling locations, nutrient data, climate data and epigenetic analyses on which
898 the present research is based, will be deposited on the data repository associated with the CREST-

899 CACHe NSF Center at Florida International University (<https://crestcache.fiu.edu/>). This center has a
900 dedicated server where data from all associated projects is deposited and made publicly available, as per
901 NSF regulations. Data will be made available to the public upon acceptance of the present work.

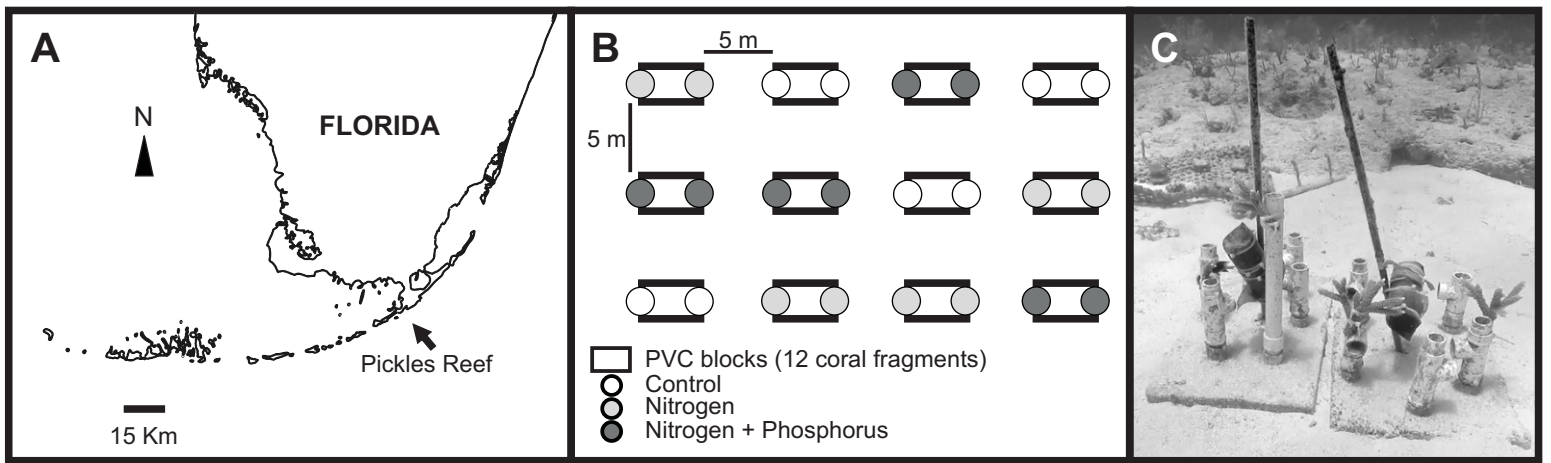


Fig. 1, Rodriguez-Casariago et al. 2018

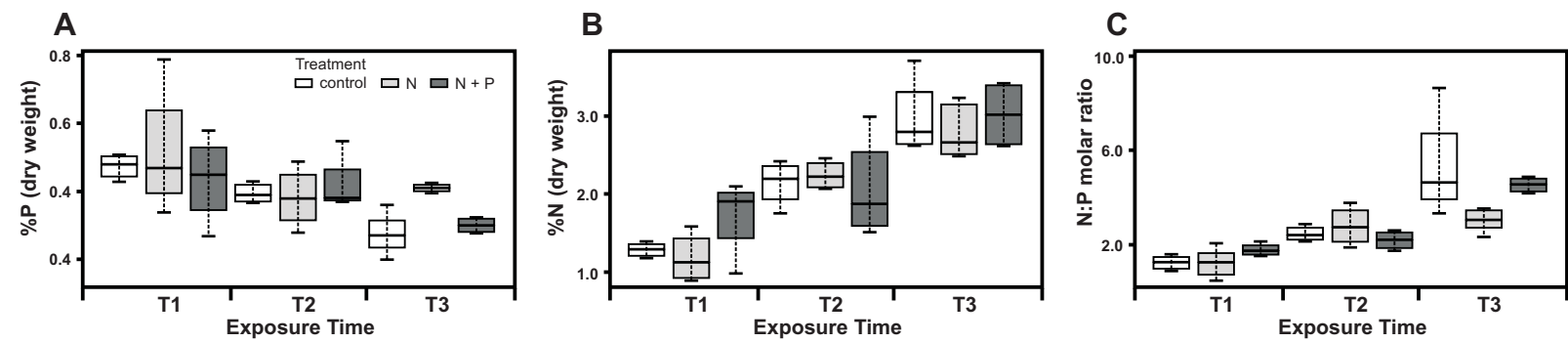


Fig. 2, Rodriguez-Casariago et al. 2018

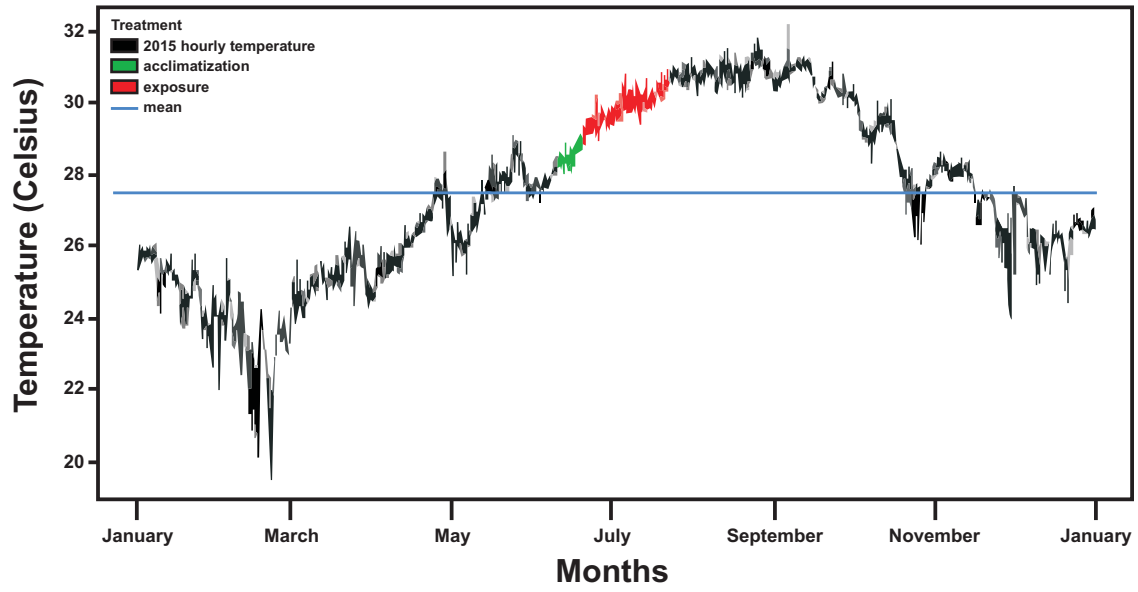


Fig. 3, Rodriguez-Casariago et al. 2018

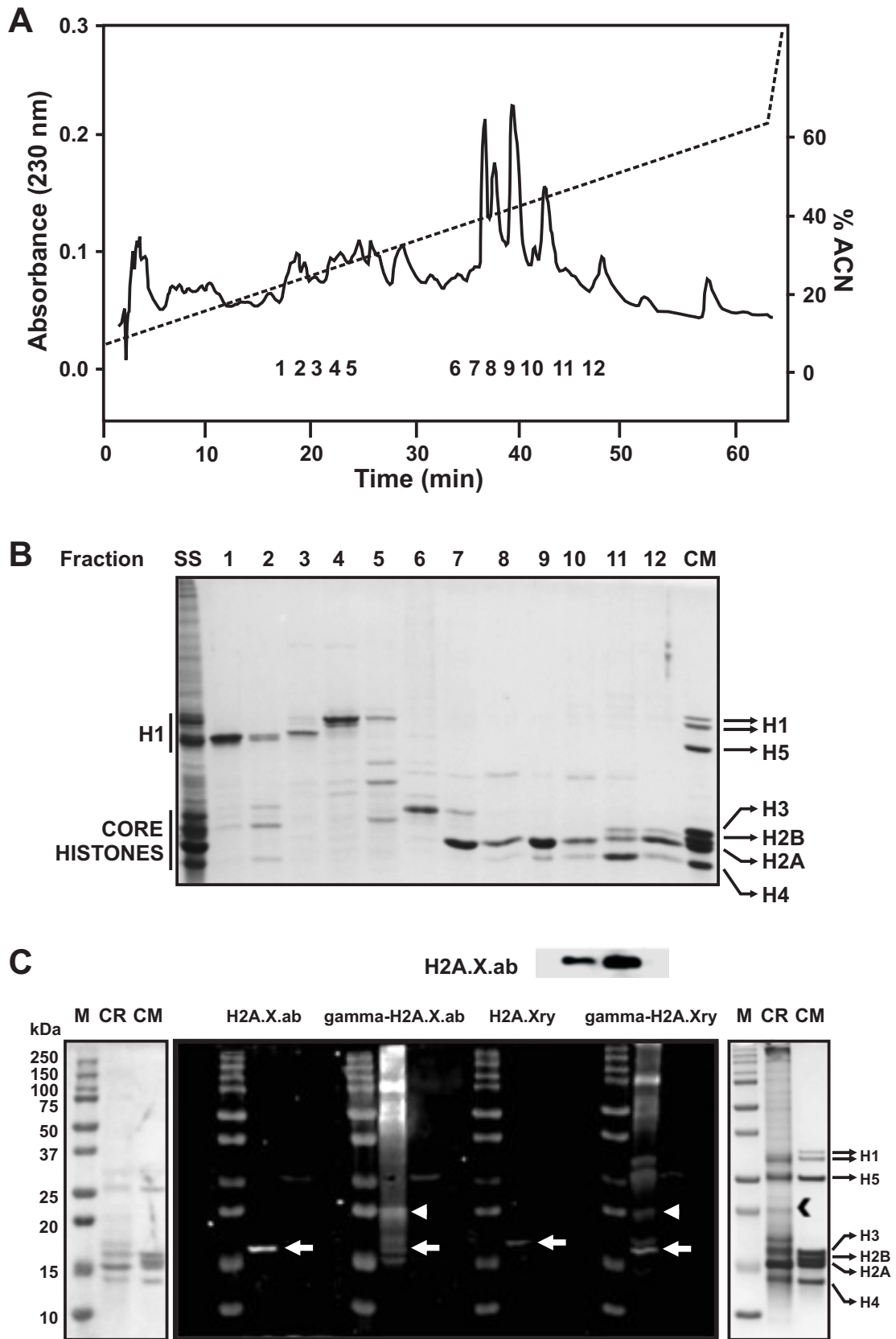


Fig. 4, Rodriguez-Casariego et al. 2018

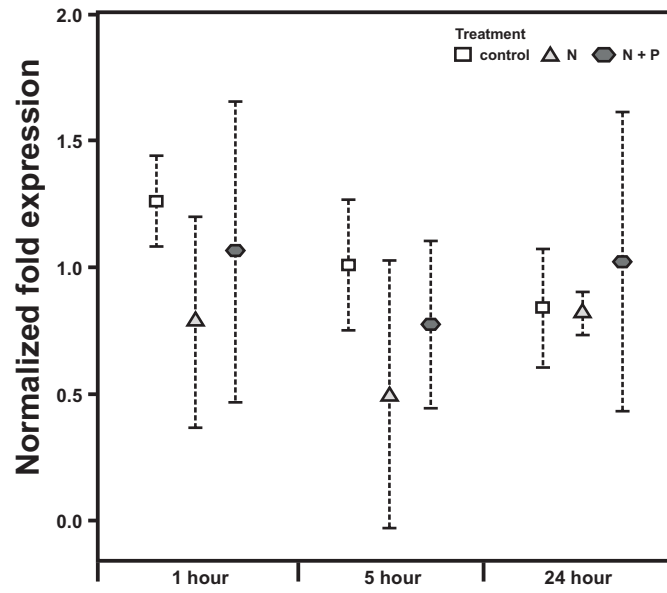


Fig. 5, Rodriguez-Casariago et al. 2018

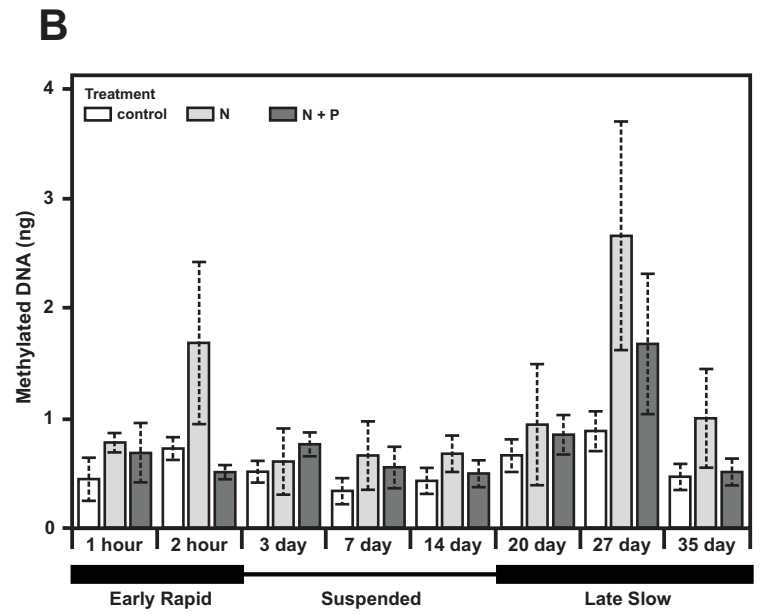
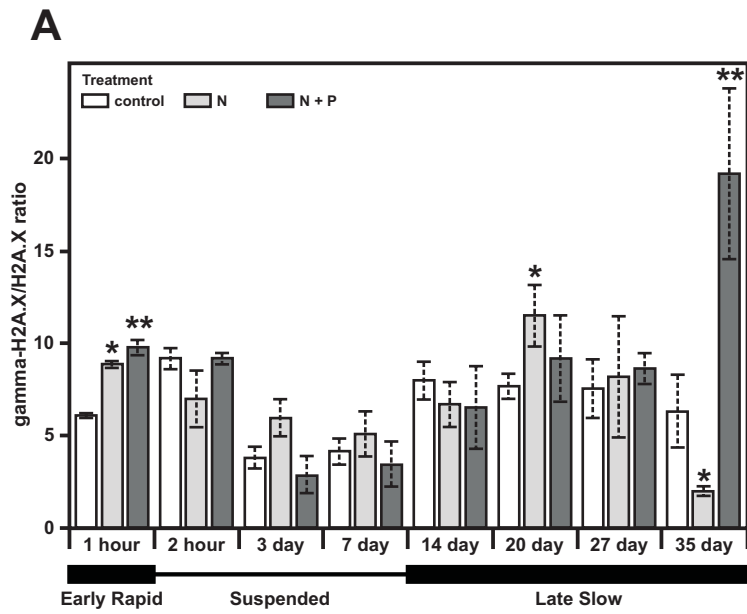
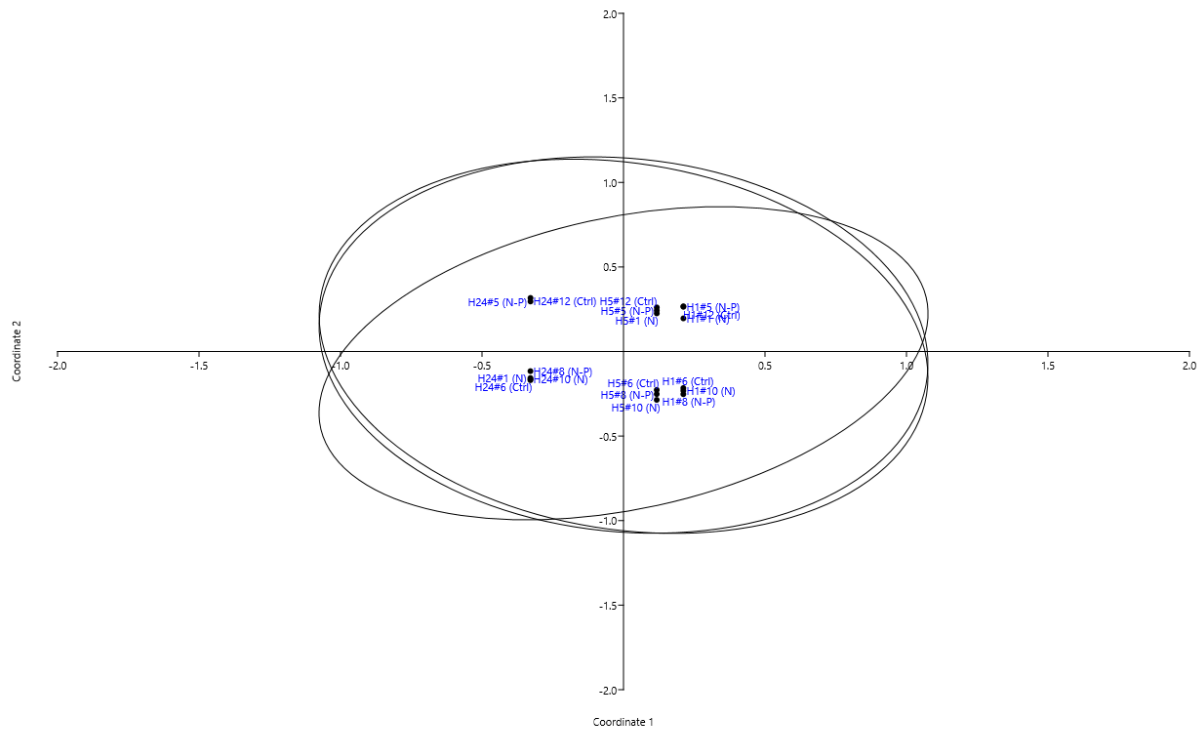


Fig. 6, Rodriguez-Casariago et al. 2018



Suppl. Fig. 1, Rodriguez-Casariago et al. 2018